Theory of interference distortion of Raman scattering line shapes in semiconductors

M. Balkanski, K. P. Jain,* R. Beserman, and M. Jouanne

Laboratoire de Physique des Solides, de l'Université Pierre et Marie Curie, associé au Centre National de la Recherche Scientifique, 4 place Jussieu, 75230 Paris Cedex 05, France

(Received 9 December 1974)

A Green's-function theory of Raman-scattering line-shape asymmetries is developed here for a system in which a one-phonon (discrete) excitation is degenerate with intervalence-band (continuum) excitations. The scattering cross section is expressed in terms of a generalized dynamic form factor, $\tilde{S}(\vec{q},\omega)$, appropriate for the second Born approximation. The $\tilde{S}(\vec{q},\omega)$ is defined in terms of a composite Green's function which describes the quantum interference between the discrete and continuum states. Introducing a model electron-phonon interaction, the techniques of many-body theory are used to solve for $\tilde{S}(\vec{q},\omega)$ in the random-phase approximation. This automatically leads to an expression which yields the desired line shapes, i.e., gives antiresonances. Measurements of scattering line shapes for degenerate p-type silicon over a wide spectral range are described. This allows a fit of the theoretical and experimental line shapes. Examination of the analytic structure of $\tilde{S}(\vec{q},\omega)$ leads to the conclusion that there is a new collective excitation of the crystal. This is the result of the quantum interference between the discrete and continuum states. We associate the creation of this excitation with the onset of line-shape asymmetry in the Raman spectrum of the semiconductor.

I. INTRODUCTION

Most one-phonon Raman-scattering (RS) experiments in semiconductors exhibit symmetric line shapes. However, recent Raman scattering experiments in degenerate p-type silicon have revealed striking and unusual effects.[1,2] It is seen that the one-phonon Raman line shape depends sensitively on a number of experimental variables, i.e., the concentration of the boron acceptors, the temperature and energy of the exciting radiation. As the number of boron acceptors or the wavelength of the incident photons increase, the one-phonon line broadens appreciably and becomes strongly asymmetric. The same effect is observed as the temperature is lowered.

The line shape of the experimental curves is suggestive. Apart from the asymmetry, there exists an antiresonance on the low-energy side of the resonance. Line shapes of this sort have been known in nuclear[3] and atomic physics[4] for a long time. The theoretical treatment of two-electron atomic resonances by Fano is particularly useful for understanding the problem in which the scattering line shape is distorted by interference between discrete and continuum eigenstates of an atom. The details of this are in Fano's paper.[4] It is sufficient here to say that the gist of the theory involves the introduction of asymmetry parameters q and Γ which can be calculated, at least, in a few simple cases for atomic systems. The function q is the ratio of the transition amplitude of the discrete state to that of the continuum states, while Γ is a measure of the strength of the coupling between the discrete and continuum states.

The first discussion of this effect in solids considered the overlap of saddle-point excitons with a continuum due to the interband electronic transitions.[5,6] Interference effects have to be invoked to fit the absorption line shapes when the oscillator strengths of these excitons is comparable to that of continuum. However, due to the complexity of the problem of Coulomb effects at hyperbolic energy surface, the analysis in Ref. 6 uses the Breit-Wigner-Fano (BWF) theory to introduce asymmetry parameters which were treated as phenomenological quantities. Success of this approach depends upon focusing attention on the antiresonances.

Previous theories of asymmetric line shapes have treated the interaction of two elementary excitations of the solid. For instance, Barker and Hopfield[7] have discussed infrared dispersion of a sharp phonon overlapping the wing of a broad phonon. These authors discuss the equations of motion in quantum-mechanical terms and then develop a classical model which illustrates the interference effects. Recent work has discussed the effect on the scattering line shapes of interaction of two optic phonons[8] and the analogous situation of plasmon-phonon interaction.[9] In all the cases cited above, a BWF interference distorts the line shapes. These and other papers concerning interference effects have been reviewed by Scott in a recent paper.[10]

It is tempting to use the BWF theory for describing Raman scattering in degenerate p-type silicon. This is because of the basic simplicity of the theory and the antiresonant behavior of the experimental line shapes. The presence of holes in p-type silicon produces an intervalence-band electronic Raman scattering. This is evident from the structure of the valence bands of silicon which consist of heavy, light hole and spin-orbit split-off bands. The main point about this process is that it gives a continuous and relatively featureless

scattering background. That is to say there are no sharp peaks in its spectrum. Of course, the electronic scattering itself is a sensitive function of the doping and the temperature. Superimposed upon this continuum is the one-phonon Raman line, which to a good approximation, may be considered to be an excitation at a single discrete energy. This statement is exact if we neglect the width due to the self-energy of the phonon. In any case, the phonon shows up as a sharp peak in the Raman scattering. The coupling between overlapping one-phonon (discrete) and electronic (continuum) Raman scattering amplitudes due to the electron-phonon interaction leads to an interference effect which manifests itself in asymmetric line shapes of the light-scattering cross section. The larger the continuum scattering relative to the discrete one, the more pronounced are the interference effects.

It must be emphasized, however, that this *ad hoc* approach is phenomenological in character and can, at best, provide rough guidelines for experimental investigations. This is because the BWF theory is only valid, strictly speaking, for nuclear or atomic states which are spatially localized. The situation for solids is quite different: Here we are dealing with spatially extended systems and propagating modes. It should also be pointed out that the BWF theory does not incorporate the effects of temperature.

In this paper we adopt a point of view more suited to the description of light-scattering line shape in semiconductors. We formulate a microscopic theory of Raman scattering from a system in which both continuum and discrete states can be excited simultaneously in a manner analogous to what was done in Refs. 8 and 9. This is different from the BWF theory since it is quantum statistical in character, while retaining the essential nature of the interference. The light-scattering cross section is expressed in terms of a generalized dynamic form factor $\tilde{S}(\vec{q}, \omega)$. The $\tilde{S}(\vec{q}, \omega)$ is a generalization of the Van Hove dynamic form factor[11] for second Born approximation to include resonance of the incident and scattered light with *intermediate* states of the scatterer (this effect is usually called resonance Raman scattering). This approach emphasizes the many-body character of the system, and we determine $\tilde{S}(\vec{q}, \omega)$ approximately using the techniques of many-body theory. The $\tilde{S}(\vec{q}, \omega)$ is itself related to a composite Green's function $F(\vec{q}, t)$, which includes the coupling between the discrete and continuum states due to the electron-phonon interaction. Introducing this interaction explicitly, we solve for $\tilde{S}(\vec{q}, \omega)$ in the random-phase approximation (RPA) by a selective summation of diagrams. This gives the desired scattering line shape automatically, which can be compared with experiments. We should add that our method has the virtue that it gives a self-consistent treatment of the spectral response of the system to the external light probe.

It emerges from the above analysis that the line-shape asymmetry is due to the onset of a composite state of the system in which it is impossible to separate the phonon and electron-hole-like character of the scattering. The exact nature of the asymmetry will, of course, be sensitive to the detailed nature of the electron-phonon interaction. In this paper we prefer to treat this as a constant, which is a fair approximation for silicon. Even with this simplification, it is evident that the line-shape asymmetry must be associated with the excitation of an eigenstate which is a new elementary excitation of the crystal due to strongly interacting phonons and electron-hole pairs. It is our contention that the beginning of the line-shape distortion signals the birth of this collective excitation. Our formulation gives not only a proper account of Raman scattering line shapes in semiconductors, but has the attractive feature that it describes a new eigenmode of a system in a natural way.

Section II presents a formulation of a microscopic theory of Raman scattering from a system in which a discrete phonon excitation is degenerate with a continuum of intervalence-band electronic excitations. The generalized dynamic form factor $\tilde{S}(\vec{q}, \omega)$ is defined in terms of a composite Green's function which describes the coupling of the discrete and continuum states. We then solve for $\tilde{S}(\vec{q}, \omega)$ within the RPA by introducing a model electron-phonon interaction. The result leads to an analysis of the scattering line shapes which also incorporates the effect of finite temperature T. By adapting the theory to the case of degenerate p-type silicon, we can express the effect of variation in line shape as a function of concentration of doping n and incident photon energy $\hbar\omega_0$.

Section III is devoted to the comparison of the theory with experimental results. We discuss the manner in which line shapes can be generated by suitable simplification of the theoretical expressions. Then we go on to describe measurements of the scattering cross section in degenerate p-type silicon. The variation of the scattering cross section with the various experimental variables, i.e., n, T, $\hbar\omega_0$ is discussed. The theoretical line shapes are compared with experimental ones and their compatibility is demonstrated for a sample set of measurements. This yields values of the electron-phonon coupling constant g. Section IV contains the discussion and concluding remarks.

II. GENERALIZED DYNAMIC FORM FACTOR

Consider the problem in which there exists a discrete phonon excitation juxtaposed on a con-

tinuum of electronic transitions between the various bands of a semiconductor. Such a situation might be expected to obtain for light scattering in p-type silicon, germanium, and III-V compounds like InSb and GaAs. In addition, it might also occur in gray tin and zero-gap semiconductors like HgTe. The theory for Raman scattering which we will present now is quite general and may be applied to a variety of experimental situations. We would be interested primarily in Raman scattering in degenerate p-type silicon. Therefore, we shall adapt our final theoretical results to make contact with our specific situation.

We introduce a composite Green's function for the whole system as follows:

$$F(\vec{q}, t) = -i\left\langle T\left(A\Phi_{\vec{q}}(t) + V^{-1}\sum_{i,j}\sum_{k} B_{ij}(\vec{k})\,\Psi_{\vec{q}}^{ij}(\vec{k}, t)\right)\right.$$
$$\left.\times\left(A\Phi_{\vec{q}}^{\dagger}(0) + V^{-1}\sum_{m,n}\sum_{\vec{k}'} B_{mn}^{*}(k')\,\Psi_{\vec{q}}^{mn}(\vec{k}', 0)\right)\right\rangle. \quad (1)$$

Here $\Phi_{\vec{q}}(t)$ are the spatial Fourier transforms of the phonon-field operators which are related to the creation and destruction operators of the phonons in the usual way,[12] and $\Psi_{\vec{q}}^{ij}(\vec{k}, t)$ the electron-hole operator which creates an electron in band i and hole in band j. The symbol T denotes the Wick time-ordering operator and the brackets $\langle\ \rangle$ indicate thermodynamic averages[13] of the operators at finite temperatures and ensemble averages at $T=0$. The functions A and B are related to the Raman tensors for one-phonon[15] (discrete) and interband electronic[14] (continuum) excitations. We must emphasize that both A and B depend upon the energy of the incoming and outgoing photons and as such describe the resonance of these photons with intermediate states.

Taking the time Fourier transform of Eq. (1), we get

$$F(\vec{q}, \omega) = A^2 F_p(\vec{q}, \omega) + V^{-2}\sum_{\substack{mn\\ij}}\sum_{\vec{k},\vec{k}'} B_{ij}^{*}B_{mn}(\vec{k}')$$
$$\times F_e^{ijmn}(\vec{k}, \vec{k}', \vec{q}, \omega)$$
$$+ 2A\,V^{-1}\sum_{ij}\sum_{\vec{k}} B(\vec{k})\,F_{ep}^{ij}(\vec{k}, \vec{q}, \omega). \quad (2)$$

Here F_p is the one-phonon Green's function, F_e that corresponding to interband electronic transitions, F_{ep} that which mixes the one-phonon and electron-hole pair states.

This form for the composite Green's function is quite general. We can simplify this formula if we neglect the effect of electron-electron interactions[14] on the $F_e^{ijmn}(\vec{k}, \vec{k}', \vec{q}, \omega)$. This is justified since we want to focus attention on interference effects. In this case we need only the $i=n$ and $j=m$ component of F_e^{ijmn}. Therefore, we define

$$F_e^{ij}(\vec{k}, \vec{k}', \vec{q}, \omega) = F_e^{ijji}(\vec{k}, \vec{k}', \vec{q}, \omega). \quad (3)$$

Further, for the sake of brevity of the notation we suppress the band indices on $F_e^{ij}(\vec{k}, \vec{k}', \vec{q}, \omega)$ and $B_{ij}(\vec{k})$, their existence being understood. We shall assume a two-valence-band model which makes the sum over i and j redundant. This assumption makes for mathematical simplicity without prejudice to the physical effects involved. Generalization to a many-valence-band model is straightforward. With these remarks, Eq. (2) becomes

$$F(\vec{q}, \omega) = A^2 F_p(\vec{q}, \omega)$$
$$+ V^{-2}\sum_{\vec{k},\vec{k}'} B(\vec{k})\,B(\vec{k}')\,F_e(\vec{k}, \vec{k}', \vec{q}, \omega)$$
$$+ 2A\,V^{-1}\sum_{\vec{k}} B(\vec{k})\,F_{ep}(\vec{k}, \vec{q}, \omega). \quad (4)$$

It is now necessary to relate $F(\vec{q}, \omega)$ to the Raman scattering cross section and for this purpose we shall make a small digression. Light scattering from the *intraband* transition of free carriers is usually described by $\vec{A}^2$ term for the electron-photon coupling, where $\vec{A}$ is the external electromagnetic vector potential.[16] In this case the differential scattering cross section for the light can, in the first Born approximation, be written as a product of the dynamic form factor $S(\vec{q}, \omega)$ and a factor which contains all the information about the incident and scatterer photons and their law of interaction with the system. The dynamic form factor $S(\vec{q}, \omega)$ contains *all* the information characteristic of the system and is determined by the particles comprising the system and their mutual interactions. This point has been stressed by Nozières[17] and enabled Van Hove[11] to relate $S(\vec{q}, \omega)$ to the Fourier transform of the time-dependent pair-distribution function for the many-body system.

Raman scattering of photons due to phonons[15] or *interband* electronic excitations[18] must be described in the second Born approximation, since the leading terms in the electron-photon coupling are $\vec{p}\cdot\vec{A}$. In this case it is no longer possible to factorize the cross section into a term which depends upon the probe and another which depends upon the target. This is because resonance of the incident and scattered light with intermediate states of the scatterer must be included. Of course, when the energy of the incident or scattered light approaches that of one of the excited states of the crystal, the resonance effect dominates and we get resonance Raman scattering.[20] However, even off-resonance, a proper theory, must include this term.[15,18] We therefore introduce a generalized dynamic form factor $\tilde{S}(\vec{q}, \omega)$, which is appropriate for the second Born approximation. This new function depends not only on the properties of the many body system but also on the energy of the

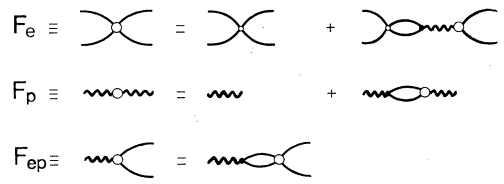

FIG. 1. Diagrammatic representation of the Green's functions F_e, F_p, and F_{ep} in the RPA. The electron-phonon interaction g is given by the small filled-in circle. The first term in the equation for F_e is its value for $g=0$. The corresponding value for the phonon propagator F_p is given by the wavy line.

incident and scattered photons.

Returning to Eq. (4), the generalized dynamic form factor is given in the region of $\omega>0$, i.e., for Stokes scattering, by

$$\tilde{S}(\vec{q},\omega) = -\operatorname{Im} F(\vec{q},\omega). \tag{5}$$

Hence to determine the cross section, we must get $F(\vec{q},\omega)$, which means solving for F_p, F_e, and F_{ep}.

It is obvious that the Green's functions are very complicated because of the many-body character of the problem. We can, therefore, hope to determine them only approximately. In this, we take recourse to standards methods of many-body theory. Before describing this, however, it is necessary to define the electron-phonon interaction for the problem at hand. For silicon because of the short range of the deformation potential,[19] it is sufficient, as a working model, to approximate the electron-phonon interaction by a constant g. It is possible to refine our subsequent treatment to include the Fröhlich interaction and anisotropy effects. We prefer to avoid this here for simplicity and because our approximation is a good one for silicon.

We now solve for the Green's functions in the RPA by a selective summation of Feynman diagrams. The diagrams to be summed are given in Fig. 1. The functions $F_e^{(0)}$ and $F_p^{(0)}$ are the electronic and phonon Green's functions in the absence of the electron-phonon interaction and g is the electron-phonon coupling constant. For $\vec{k}=\vec{k}'$, the $F_e^{(0)}$ is given by[14]

$$F_e^{(0)}(\vec{k},\vec{k}',\vec{q},\omega) = [f_i(\vec{k}) - f_j(\vec{k}+\vec{q})] \times [E_i(\vec{k}) - E_j(\vec{k}+\vec{q}) + \hbar\omega + i\eta]^{-1}, \tag{6}$$

where $E_i(\vec{k})$ is the electron energy, $f_i(\vec{k})$ the corresponding Fermi factor, and $\eta\to 0$. For the phonons we use (for $T=0$)

$$F_p^{(0)}(\vec{q},\omega) = [\omega - \omega_p(\vec{q}) + i\eta]^{-1} - [\omega + \omega_p(\vec{q}) - i\eta]^{-1}, \tag{7}$$

where $\omega_p(\vec{q})$ is the unperturbed phonon frequency. We prefer to use the $T=0$ form of $F_0^{(0)}$ and avoid the complications of its finite-temperature counterpart. This is reasonable since, as will be discussed later, the effect of T on $F_p^{(0)}$ is small. From Fig. 1 we get the Green's function

$$F_e(\vec{k},\vec{k}',\vec{q},\omega) = F_e^{(0)}(\vec{k},\vec{k}',\vec{q},\omega) + \frac{g^2\Lambda^{(0)}(\vec{k},\vec{q},\omega)\,F_p^{(0)}(\vec{q},\omega)\,\Lambda^{(0)}(\vec{k}',\vec{q},\omega)}{1-g^2\Delta^{(0)}(\vec{q},\omega)\,F_p^{(0)}(\vec{q},\omega)}, \tag{8}$$

$$F_p(\vec{q},\omega) = \frac{F_p^{(0)}(\vec{q},\omega)}{1-g^2\Delta^{(0)}(q,\omega)\,F_p^{(0)}(\vec{q},\omega)}, \tag{9}$$

and

$$F_{ep}(\vec{k},\vec{q},\omega) = \frac{g\,F_p^{(0)}(\vec{q},\omega)\,\Lambda^{(0)}(\vec{k},\vec{q},\omega)}{1-g^2\Delta^{(0)}(\vec{q},\omega)\,F_p^{(0)}(\vec{q},\omega)}. \tag{10}$$

Here

$$\Lambda^{(0)}(\vec{k},\vec{q},\omega) = \sum_{\vec{k}'} F_e^{(0)}(\vec{k},\vec{k}',\vec{q},\omega) \tag{11}$$

and

$$\Delta^{(0)}(\vec{q},\omega) = \sum_{\vec{k},\vec{k}'} F_e^{(0)}(\vec{k},\vec{k}',\vec{q},\omega). \tag{12}$$

Using Eqs. (4) and (8)–(10) we get for the composite Green's function

$$F(\vec{q},\omega) = \tilde{F}_p(\vec{q},\omega) + \tilde{F}_e(\vec{q},\omega) + 2\tilde{F}_{ep}(\vec{q},\omega), \tag{13}$$

where

$$\tilde{F}_p(\vec{q},\omega) = A^2 F_p(\vec{q},\omega), \tag{14}$$

$$\tilde{F}_e(\vec{q},\omega) = \sum_{\vec{k},\vec{k}'} B(\vec{k})\,B^*(\vec{k}')\,F_e(\vec{k},\vec{k}',\vec{q},\omega), \tag{15}$$

and

$$\tilde{F}_{ep}(\vec{q},\omega) = A\sum_{\vec{k}} B(\vec{k})\,F_{ep}(\vec{k},\vec{q},\omega). \tag{16}$$

Combining Eqs. (5) and (13)–(16) we get the following expression for the generalized dynamic form factor:

$$\tilde{S}(\vec{q},\omega) = (A^2/|G|^2)(F_p'G'' - F_p''G') - \tilde{F}_e'' + g^2\{G''[F_p'(\tilde{\Lambda}'^2 - \tilde{\Lambda}''^2) - 2F_p''\tilde{\Lambda}'\tilde{\Lambda}''] - G'[2F_p'\tilde{\Lambda}'\tilde{\Lambda}'' + F_p''(\tilde{\Lambda}^2 - \tilde{\Lambda}''^2)]\}/|G|^2 + 2Ag[G''(F_p'\tilde{\Lambda}' - F_p''\tilde{\Lambda}'') - G'(F_p''\tilde{\Lambda}' + F_p'\tilde{\Lambda}'')]/|G|^2, \tag{17}$$

with

$$G' = 1 - g^2(\Delta' F_p' - \Delta'' F_p''), \tag{18}$$

$$G'' = -g^2(\Delta' F_p'' + \Delta'' F_p'), \tag{19}$$

and

$$\tilde{\Lambda}(\vec{q}, \omega) = \sum_{\vec{k},\vec{k}'} B(\vec{k})\, F_e^{(0)}(\vec{k}, \vec{k}', \vec{q}, \omega). \tag{20}$$

In Eqs. (17)–(19) it is understood that all the functions depend upon $\vec{q}$ and ω. Further, we have suppressed the superscripts on $F_e^{(0)}$, $F_p^{(0)}$, and $\Delta^{(0)}$, it being implicit that they refer to the noninteracting case. The superscript prime denotes the real part of a function, and double prime its imaginary part. Equation (17) is the most general result in this paper, and the RS line shape, is determined by it.

The complicated look of the above set of equations makes it necessary to point out the salient features for insight into their structure. The terms $\tilde{F}_p(\vec{q}, \omega)$ and $\tilde{F}_e(\vec{q}, \omega)$ in Eq. (13) give the scattering from phonon and interband electronic excitations appropriately renormalized by the electron-phonon interaction. The denominators of Eqs. (9) and (10) and hence of $\tilde{F}_p(\vec{q}, \omega)$ and $\tilde{F}_e(\vec{q}, \omega)$ are typical of RPA calculations where a geometric series is summed. The term $\tilde{F}_{ep}(\vec{q}, \omega)$ is the "interference" between the phonons and continuum electronic states and it vanishes when $g \to 0$, as it should. This is the term, which is primarily responsible for distorting the line shape. It should be emphasized that this "interference" incorporates the interference of the BWF theory while expressing the effect in terms of Green's functions. This is obviously appropriate for describing scattering line shape in solids.

We can gain further insight into the structure of Eq. (17) by regrouping various terms in it. The coupling constant g is a measure of the interaction between phonons and electrons in particular bands from which originate the continuum of electronic transitions. It is not known how this coupling constant compares with coupling constants of phonons with the electrons in other bands which are, for example, implicit in the function A. It is therefore expedient to introduce a general electron-phonon coupling constant λ for the interaction between phonons and all electrons in the crystal. All the deformation-potential constants which are defined by taking appropriate matrix elements of the electron-phonon interaction Hamiltonian are proportional to λ. As there is no *a priori* information about the relative magnitude of these different deformation potentials, we can classify different terms in the calculation in powers of λ. Consequently, since $A(\omega) \sim \lambda$ and $g \sim \lambda$, Eq. (17) expresses $\tilde{S}(\vec{q}, \omega)$ correct to second order in λ. It is shown in the Appendix that Eq. (17) can be written

$$\tilde{S}(\vec{q}, \omega) = -\tilde{F}_e'' - [(A + g\tilde{\Lambda}')^2 - g^2\tilde{\Lambda}''^2] \times F_p'' - 2(A + g\tilde{\Lambda}')\, g\tilde{\Lambda}'' F_p', \tag{21}$$

where F_p is given by Eq. (9). Further, by simple algebraic manipulation, it is shown in the Appendix that

$$\tilde{S}(\vec{q}, \omega) = -\tilde{F}_e'' + \sigma_0[(q + \epsilon)^2/(1 + \epsilon^2)] - \sigma_0, \tag{22}$$

where the functions q, ϵ, and σ_0 are also defined.

It will be seen that the second term of the above equation is just the Fano[4] line-shape function multiplied by σ_0. In fact, writing Eq. (22) as

$$\tilde{S}(\vec{q}, \omega) = -\tilde{F}_e'' + [(q^2 - 1)/(1 + \epsilon^2)]\sigma_0 + [2q\epsilon/(1 + \epsilon^2)]\sigma_0, \tag{23}$$

it is easy to see that the second terms of Eqs. (21) and (23) are equal to each other and represent the RS from the modified discrete state. The third terms of these equations give the contribution due to interference between the discrete and continuum states while the first terms are due to interband electronic transitions. It must be stressed that Eq. (22) allows for both partial and complete antiresonances. The latter situation obtains if $|\tilde{F}_e''| = |\sigma_0|$. The positive definiteness of the scattering cross section is guaranteed by the unitarity of the S matrix and does not have to be imposed arbitrarily. This implies that $|\tilde{F}_e''| \geq |\sigma_0|$.

The pole of $F(\vec{q}, \omega)$ corresponds to the real elementary excitations of the system. Neglecting the damping of the phonon by other processes, the energy of the excitations ω_R is given by the solution of the equation

$$g^2\Delta'(\vec{q}, \omega_R)\, F_p'(\vec{q}, \omega_R) = 1, \tag{24}$$

which also gives the dispersion of these modes. Neglecting the dispersion, Eq. (24) reduces (for emission of phonons) to

$$g^2\Delta'(\omega_R)\,(\omega_R - \omega_p)^{-1} = 1, \tag{25}$$

where ω_R is the new excitation frequency and ω_p the unperturbed phonon frequency. Since $\Delta'(\omega)$ is a slowly varying function of ω; we get for small g,

$$\omega_R \simeq \omega_p + g^2\Delta'(\omega_p). \tag{26}$$

From the above arguments it is clear that if the interaction is weak, the phonon pole is shifted by a small amount because of discrete-continuum self-energy effects, which brings out the quasiparticle character of the excitations. In addition to a simple pole of the phonon, there exists a branch cut in the complex ω plane due to the continuum of interband electronic transitions which overlaps with it. This is evident from the structure of Eq. (24). The analytic structure of $F(\vec{q}, \omega)$ illustrates how the coupling of the discrete-continuum excitations affects the RS. As long as

the coupling of the discrete-continuum is weak, we still have a phononlike pole as explained above and the strength of the scattering is given by its residue. The residue diminishes as the coupling increases, i.e., the discrete state is displaced and dissolved in the continuum by the interaction. As the coupling is increased even further, the phononlike character of the excitation disappears and we have a mixed mode of the crystal. For very large coupling the resonance disappears and we are only left with an antiresonance. We shall return to this point later. It is necessary to emphasize that the line shape is determined by the $\tilde{S}(\vec{q}, \omega)$, which is the spectral function of the Lehmann representation for $F(\vec{q}, \omega)$,[17] rather than by the poles of $F(\vec{q}, \omega)$ The latter only define the resonant energies and lifetimes of the quasiparticle excitations.

It is evident from the definition of $F_e^{(0)}$ and $F_p^{(0)}$ [see Eqs. (6) and (7)] that the line shape depends upon the temperature T and the concentration of doping n. The point is that the intervalence-band electronic RS is very sensitive to the concentration and temperature—particularly for p-type silicon. This fact is amply substantiated by experimental evidence and its detailed analysis.[21] The variation of electronic RS with n comes in through the chemical potential μ in the Fermi functions. As n increases, $|\mu|$ increases and together with the intervalence-band structure of silicon, this leads to an overall enhancement of the electronic RS.[21] The effect of n on $F_p^{(0)}$ is very weak. Turning to the effect of the temperature, again the Fermi functions play the main role through μ. As T decreases, $|\mu|$ increases and we have for silicon an enhancement of the electronic RS. Again the effect of T on $F_p^{(0)}$ is weak,[22] relative to the electronic RS. This means that as n increases or T decreases, the electronic RS increases with respect to phonon RS and interference effects begin to predominate. These qualitative remarks make the compatibility of the theory given here and experiment seem plausible. A thorough examination of this is given in Ref. 21 which establishes the correctness of our approach.

Before concluding this section, a few words about the dependence of RS line shape on the energy of the incident radiation $\hbar\omega_0$ are in order. This comes in through the functions A and B. The line shape is determined by Eq. (22), which depends upon A and B [through $\tilde{\Lambda}(\vec{q}, \omega)$]. We may argue roughly as follows. For the phonons,[15] at least for the M_0 edge and neglecting electron-hole interaction, we have

$$A(\omega_0) \sim (\omega_g + \omega - \omega_0)^{1/2} - (\omega_g - \omega_0)^{1/2}, \tag{27}$$

where $\hbar\omega_g$ is the band-gap energy. For the interband electronic RS, the resonance is controlled by[18]

$$B(\omega_0) \sim (\omega_g + \alpha\omega - \omega_0)^{-1} - (\omega_g + \alpha\omega + \omega_0)^{-1}, \tag{28}$$

where α is an adjustable parameter, which takes into account the unknown $\vec{k}$-dependence band structure.

As the energy of the incident photon approaches that of one of the gaps, $A(\omega_0)$ increases more rapidly than $B(\omega_0)$ because of the high value of α. This weakens the interference effects,[21] which is in agreement with experimental results.

III. COMPARISON OF THEORETICAL AND EXPERIMENTAL LINE SHAPES

We have discussed the underlying theory of line-shape distortion due to discrete-continuum interaction at length in Sec. II. It is our purpose here to simplify the complicated expression for $\tilde{S}(\vec{q}, \omega)$ [Eq. (22)] with approximations which can be justified on physical grounds. Then, the line shapes generated from the simplified expression for $\tilde{S}(\vec{q}, \omega)$ can be fitted to some of the measured ones. We must point out that our aim here is strictly limited: We wish to demonstrate the correctness of our approach. A complete analysis of the general form for $\tilde{S}(\vec{q}, \omega)$ vis-à-vis the over-all experimental results will be published elsewhere.[21]

Consider the functions in Eq. (22) which come from interband electronic RS. These are Δ, $\tilde{F}_e$, and $\tilde{\Lambda}$. The structure of $\tilde{F}_e''$ has been studied before for gray tin[18] and interband transitions in the valence bands for groups IV and III-V compounds.[14] Using an effective-mass approximation and noting that $\vec{k} = \vec{k}'$, we do the sum over $|\vec{k}|$ and get (for optical experiments, we have $\vec{q} = 0$)

$$\tilde{F}_e(\vec{q} = 0, \omega) \sim \frac{\omega_0}{\omega_1} \omega^{1/2} \int d\Omega(\vec{k}) \quad (\text{function of } \vec{k}). \tag{29}$$

The explicit form of the function of $\vec{k}$ is given in Ref. 18 and depends upon ω and ω_0 through energy denominators. The actual numerical value of the angular integral in Eq. (29) depends on the specific material and the scattering geometry and requires the knowledge of the wave functions near $\vec{k} = 0$. It is beyond the scope of this paper to perform the angular integrals to determine $\tilde{F}_e$ and $\tilde{\Lambda}$ for silicon. We simply assume that $B(\vec{k})$ is independent of $\vec{k}$. Then from Eqs. (12), (15), and (20) we get

$$\tilde{F}_e(\omega) \simeq B^2(\omega)\Delta(\omega) \tag{30}$$

and

$$\tilde{\Lambda}(\omega) \simeq B(\omega)\Delta(\omega) . \tag{31}$$

With this assumption, the generalized dynamic form factor becomes

$$\tilde{S}(\vec{q} = 0, \omega) = \sigma_0(q + \epsilon)^2/(1 + \epsilon^2) , \tag{32}$$

where

$$q = -(A + gB\Delta')/gB\Delta'' \qquad (33)$$

and σ_0 and ϵ are changed appropriately from their definitions in the Appendix. Equation (32) is the simplest form of $\tilde{S}(\vec{q}=0, \omega)$ which can be compared with experiments and in this paper we shall confine our attention to it. The main point to note about the Fano-type formula [Eq. (32)] is that the line-shape asymmetry is determined by the function q. Since the electronic functions Δ', Δ'', and the intensity functions A and B vary weakly with energy $\hbar\omega$, so will q. Now $\Delta'' < 0$, as well as Δ' for $\omega \simeq \omega_R$. In either case, if $|A| > |gB\Delta'|$, Eq. (33) gives an antiresonance ($q > 0$) on the low-energy side of the resonance for $g > 0$, which is consistent with experimental results. The sign of the electron-phonon interaction is as it should be. For large values of the asymmetry parameter q, the line is symmetric. This happens when the transition amplitude of the electronic continuum background is small compared to that of phonon resonance. At the other extreme, for small q the line is very asymmetric and the antiresonances deep. It should be pointed out that Eq. (32) gives perfect antiresonances, which is a consequence of the approximations made in Eqs. (30) and (31). In actual fact this may not be quite so, but it is nevertheless expected that the parameter q will be a good index of line-shape asymmetry.

The qualitative Raman spectrum of heavily doped silicon has been reported previously.[1,2] We have performed experiments to include the electronic RS and the comparative intensities of the spectrum as a function of the free-carrier concentration, laser wavelength, and temperature. A complete report of our experimental results will be published elsewhere.[21]

The exciting sources were the 6471-Å line of the Coherent Radiation 52K krypton-ion and 4880-Å line of the Spectra Physics Argon-ion lasers. The analyzing spectrometer was a Coderg PHO 800-mm double monochromator and a photon counting system. To compare the scattering intensities, measurements were made with respect to a standard which was taken as the 110-cm^{-1} air line. In the backscattering configuration the best results were obtained for the incident laser beam at the Brewster angle to the sample surface. With this geometry there is no reflected light and this allows measurements close to the Rayleigh line. The surface sample was perpendicular to the $\langle 111 \rangle$ direction and due to the high index of refraction, the incident and scattered wave vectors were parallel to the $\langle 111 \rangle$ axis. The free-carrier concentration was inferred from the infrared reflectivity plasma frequency.

In Fig. 2 we show the hand-smoothed traces of the Raman spectrum of pure silicon, silicon containing 7.6×10^{19}, 1.13×10^{20}, and 2.7×10^{20} B ions/cm^3. The experiment was done at room temperature with the 4880-Å laser line. It is seen that the asymmetry of the resonance line as well as the electronic RS increases with increasing doping.

The functions $B(\omega)$, $\Delta'(\omega)$, and $\Delta''(\omega)$ pertaining to the electronic RS were determined in the following way. The energy dependence of the electronic RS may be written[18]

$$B^2(\omega)\Delta''(\omega) \sim (\hbar\omega)^{1/2}(\hbar\omega_g + \alpha\hbar\omega - \hbar\omega_0)^{-2}, \qquad (34)$$

where α is a fitting parameter to take into account the unknown $\vec{k}$ dependence of the bands. A fit of Eq. (34) with the experimental curves determines α and the energy dependence of $B(\omega)$. Figure 3 shows the fit of the experimental electronic RS with Eq. (34). The experimental electronic RS is obtained by subtracting the multiphonon contributions of the pure-silicon intensity from that of the doped silicon for frequencies outside the inter-

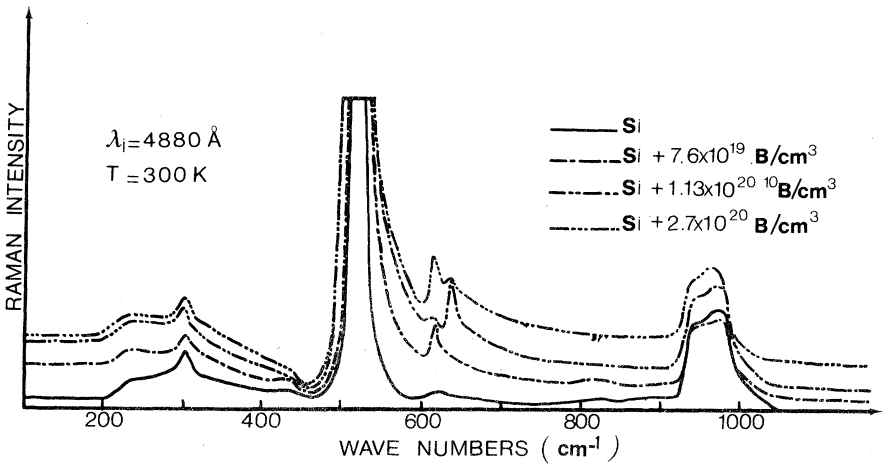

FIG. 2. Raman scattering spectra of silicon containing different concentrations of boron, with the 4880-Å laser, at room temperature.

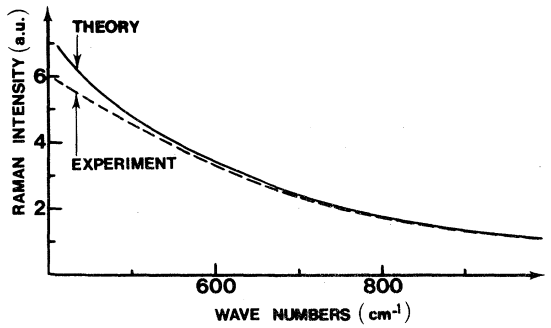

FIG. 3. Electronic Raman scattering, comparison between theory [Eq. (34)] and experiment extrapolated from the noninteracting range.

ference region. The contribution in the interference region is obtained by extrapolation. The actual value of $B(\omega)$ was obtained by using the theoretical expression for $\Delta''(\omega)$ and fitting the product $B^2(\omega)\Delta''(\omega)$ to the experimentally observed cross sections for the electronic RS.

The function $A(\omega)$ for the phonon RS was determined from the spectrum of pure silicon and a value of $\omega_p = 520.5$ cm^{-1} was used in the expression for ϵ.

The theoretical line shapes were generated by using Eq. (32). The results of this are given in Fig. 4, for one exciting laser wavelength 6471 Å at 2.4 K, which also shows their fit with the experimental line shapes. It is evident that there is good agreement between the theory and the experiment, for two impurity concentrations: 1.13×10^{20} and 3.3×10^{20} ^{10}B cm^{-3}. The value of the new excitation half-width is $\Gamma = 10 \pm 0.5$ cm^{-1}.

IV. DISCUSSION AND CONCLUDING REMARKS

We have shown in Sec. III how the RS line shapes in degenerate p-type silicon can be fitted to the experimentally observed ones. The important thing to notice about this fit is that Eq. (17) for $\tilde{S}(\tilde{q}, \omega)$ and its simplified form Eq. (32) can be expressed in terms of Green's functions for a system of noninteracting phonons and electron-hole pairs. This means that we can determine the phonon Green's function by using the measured cross section for pure silicon. The Green's function of the electron-hole pair is determined in a region far away from the resonance, where the scattering is purely electronic, and then extrapolated to the resonance region. This approach has the virtue that there is only *one* disposable parameter in the fit, which is the electron-phonon coupling strength g. We verify that g is a constant independent of $\hbar\omega_0$ and n because Γ and Δ'' do not depend on these quantities.

Throughout our treatment, the effect of temperatures has been incorporated into the theory in a self-consistent manner. This is because of the quantum-statistical nature of our approach. As already stated, the electron-hole Green's function is a sensitive function of the temperature. This is less so for the phonon Green's function, where the temperature would come in through a Bose factor and width Γ_p due to anharmonic interaction between phonons. As T increases, Γ_p increases. One way in which the temperature could be introduced into

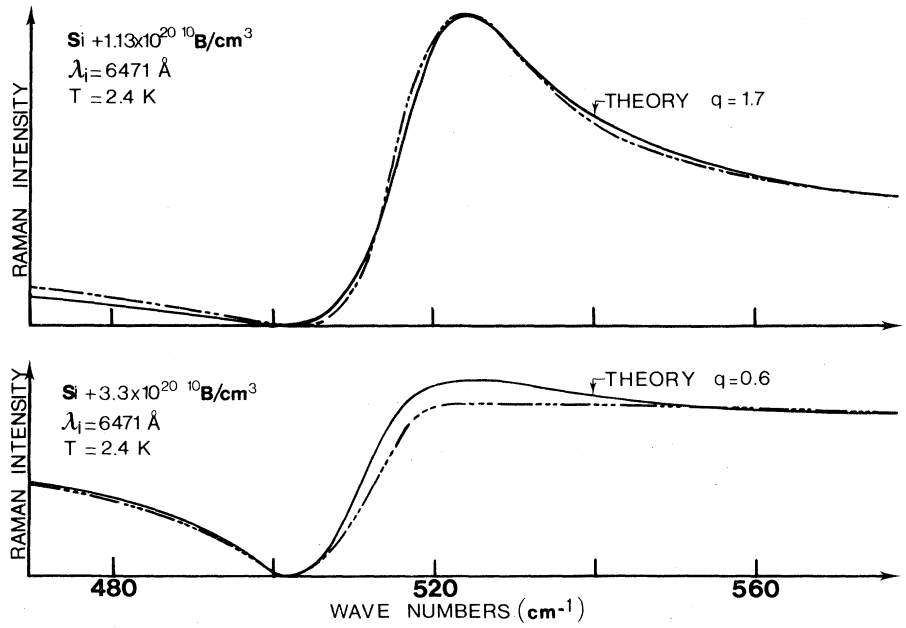

FIG. 4. Comparison of the theory Eq. (32) and experiment for Si+1.13×10^{20} B atoms/cm^3 and Si+3.3×10^{20} B atoms/cm^3 with $\lambda_{laser} = 6471$ Å, the full line is the theory and the dashed is the experiment.

the BWF treatment of the problem is to consider the phonon self-energy due to phonon-phonon interaction as giving an incoherent broadening Γ_p. Then the final line shape could be generated by convoluting[6] the Fano formula with a Gaussian of width Γ_p. This approach would neglect the effect of T on the interband electronic scattering, which we know is important. Our formulation avoids this procedure and gives a proper account of the temperature dependence of the scattering. Further, the theory also adequately describes the variation of the spectrum with the concentration of doping and energy of the incident photons.

An important by-product of our theory is the natural way in which the line-shape asymmetry can be correlated to a new collective excitation of the system. The asymmetry is a direct consequence of the coupling of discrete and continuum states. The same interaction leads to a composite state of the crystal which is collective and bosonlike in character and which we propose to name interferon. In fact, we may give a spectroscopic criterion for this new state: the line-shape asymmetry is an index of the formation of the collective excitation. The oscillator strength of this excitation is determined by the residue of the pole which defines it. The value of the residue would depend upon the phase relationship between the discrete and continuum scattering amplitude and their relative magnitudes. Turning to the concomitant antiresonance, we see that this is a consequence of the destructive interference. When the electronic RS is weak, antiresonances are difficult to detect and may be masked by incoherent broadening. As the oscillator strength of the electronic RS increases, i.e., by increasing the doping, antiresonances become more evident. Eventually, for high enough doping the resonance all but disappears leaving only the antiresonance. At this point the residue of the resonance pole is almost zero.

We conclude by stating that although the above analysis has focused attention on a phonon coupling to electron-hole excitations, the theory developed above is quite general. It might be expected to apply to a variety of situations in which overlapping discrete and continuum states interact strongly. Appropriate discrete-continuum coupling would have to be introduced for each case. The general approach and structure of the theory would be the same as that presented above.

APPENDIX

The set of Eqs. (8)–(10) can be written

$$F_p(\vec{q},\omega)=\frac{F_p^{(0)}(\vec{q},\omega)}{1-g^2\Delta^{(0)}(\vec{q},\omega)F_p^{(0)}(\vec{q},\omega)}, \tag{A1}$$

$$F_e(\vec{q},\omega)=F_e^{(0)}(\vec{k},\vec{k}',\vec{q},\omega) + g^2\Lambda^{(0)}(\vec{k},\vec{q},\omega)F_p(\vec{q},\omega)\Lambda^{(0)}(\vec{k}',\vec{q},\omega), \tag{A2}$$

and

$$F_{ep}(\vec{q},\omega)=g\Lambda^{(0)}(\vec{k},\vec{q},\omega)F_p(\vec{q},\omega)\,. \tag{A3}$$

Combining these and Eqs. (13)–(16) we get

$$F(\vec{q},\omega)=[\tilde{F}_e^{(0)}(\vec{q},\omega)+A+g\tilde{\Lambda}(\vec{q},\omega)]^2F_p(\vec{q},\omega)\,, \tag{A4}$$

which leads to Eq. (21) for $\tilde{S}(\vec{q},\omega)$. For Stokes scattering ($\omega>0$) at $T=0$,

$$F_p^{(0)}(\omega)=(\omega-\omega_p+i\delta)^{-1}, \tag{A5}$$

so that

$$F_p(\omega)=(\omega-\omega_R+i\Gamma)^{-1}, \tag{A6}$$

where the new excitation frequency and width are given, respectively, by

$$\omega_R=\omega_p+g^2\Delta^{(0)\prime} \tag{A7}$$

and

$$\Gamma=-g^2\Delta^{(0)\prime\prime}\,. \tag{A8}$$

We now write F_p' and F_p'' as

$$F_p'=\Gamma^{-1}[\epsilon/(\epsilon^2+1)] \tag{A9}$$

and

$$F_p''=-\Gamma^{-1}[1/(\epsilon^2+1)], \tag{A10}$$

where we have introduced the reduced energy variable

$$\epsilon=(\omega-\omega_R)/\Gamma\,. \tag{A11}$$

With these, and introducing the functions q and σ_0 by

$$q=-(A+g\tilde{\Lambda}')/g\tilde{\Lambda}'' \tag{A12}$$

and

$$\sigma_0=g^2\tilde{\Lambda}''^2/\Gamma=-\Lambda''^2/\Delta^{(0)\prime\prime}, \tag{A13}$$

the generalized dynamic form factor becomes using Eq. (A4):

$$\tilde{S}(\vec{q},\omega)=-\tilde{F}_e^{(0)\prime\prime}+\sigma_0(q+\epsilon)^2/(1+\epsilon^2)-\sigma_0\,. \tag{A14}$$

This is a typical Fano-type formula.

---

*Permanent address: Physics Dept., Indian Institute of Technology, New Delhi 29, India.

[1]R. Beserman, M. Jouanne, and M. Balkanski, in *Proceedings of the Eleventh International Conference on the Physics of Semiconductors, Warsaw*, 1972 (Polish Scientific Publ., Warsaw, 1972), p. 1181.

[2]F. Cerdeira, T. A. Fjeldly, and M. Cardona, Phys. Rev. B 8, 4734 (1973).

[3]G. Breit and E. Wigner, Phys. Rev. 49, 519 (1936).
[4]U. Fano, Phys. Rev. 124, 1866 (1961).
[5]J. C. Phillips, Phys. Rev. Lett. 12, 447 (1964).
[6]K. P. Jain, Phys. Rev. 139, A544 (1965).
[7]A. S. Barker and J. J. Hopfield, Phys. Rev. 135, A1732 (1964).
[8]A. Zawadowski and J. Ruvalds, Phys. Rev. Lett. 24, 1111 (1970); J. Ruvalds and A. Zawadowski, Phys. Rev. B 2, 1172 (1970).
[9]J. F. Scott, J. C. Damen, J. Ruvalds, and A. Zawadowski, Phys. Rev. B 3, 1295 (1971).
[10]J. F. Scott, Rev. Mod. Phys. 46, 83 (1974).
[11]L. Van Hove, Phys. Rev. 95, 249 (1954).
[12]See, for example, J. R. Schrieffer, *Theory of Superconductivity* (Benjamin, New York, 1964).
[13]G. Baym and L. P. Kadanoff, *Quantum Statistical Mechanics* (Benjamin, New York, 1962).
[14]D. L. Mills, R. F. Wallis, and E. Burstein, in *Proceedings of the Second International Conference on Light Scattering in Solids*, edited by M. Balkanski (Flammarion, Paris, 1971), p. 107.
[15]R. Loudon, Proc. R. Soc. A 275, 218 (1963).
[16]P. A. Wolff, in *Light Scattering in Solids*, edited by G. B. Wright (Springer, New York, 1969), p. 273.
[17]P. Nozières, *Theory of Interacting Fermi System* (Benjamin, New York, 1963).
[18]E. Burstein, D. L. Mills, and R. F. Wallis, Phys. Rev. B 4, 2429 (1971).
[19]G. L. Bir and G. E. Pikus, Fiz. Tverd. Tela 2, 2287 (1960) [Sov. Phys.-Solid State 2, 2039 (1961)].
[20]A. K. Ganguly and J. L. Birman, Phys. Rev. 162, 806 (1967).
[21]M. Jouanne, R. Beserman, K. P. Jain, and M. Baklanski, Phys. Rev. B (to be published).
[22]Anharmonic interactions give line broadening as the temperature is increased. This effect is very small compared to the interference effects for determining the line shapes.